Title
Localized Evaporative Cooling Explains Observed Ocular Surface-Temperature Patterns.

Journal
Investigative Ophthalmology & Visual Science, 65(10)

Authors
Kim, Young
Lee, Joshua
Yi, Sarah
et al.

Publication Date
2024-08-01

DOI
10.1167/iovs.65.10.15

Peer reviewed

Localized Evaporative Cooling Explains Observed Ocular Surface-Temperature Patterns

Young Hyun Kim,[1–3] Joshua Lee,[2] Sarah M. Yi,[3,4] Meng C. Lin,[1,3] and Clayton J. Radke[1,2]

[1]Herbert Wertheim School of Optometry & Vision Science, University of California – Berkeley, Berkeley California, United States
[2]Chemical and Biomolecular Engineering Department, University of California – Berkeley, Berkeley, California, United States
[3]Clinical Research Center, Herbert Wertheim School of Optometry & Vision Science, University of California – Berkeley, Berkeley, California, United States
[4]Department of Medicine, Emory School of Medicine, Emory University, Atlanta, Georgia, United States

Correspondence: Clayton J. Radke, Department of Chemical and Biomolecular Engineering, University of California – Berkeley, 101E Gilman Hall, Berkeley, CA 94720-1462, USA; radke@berkeley.edu.

Received: May 2, 2024
Accepted: July 18, 2024
Published: August 7, 2024

Citation: Kim YH, Lee J, Yi SM, Lin MC, Radke CJ. Localized evaporative cooling explains observed ocular surface-temperature patterns. *Invest Ophthalmol Vis Sci.* 2024;65(10):15. https://doi.org/10.1167/iovs.65.10.15

Purpose. We determined interblink corneal surface-temperature decline and tear-film evaporation rates of localized tear breakup cold regions (LCRs) and localized tear unbroken warm regions (LWRs) of the corneal surface, as well as that of the overall average corneal surface.

Methods. Each subject underwent 4 inter-day visits where the interblink corneal surface-temperature history of the right eye was measured using a FLIR A655sc infrared thermographer. Corneal surface temperature history was analyzed to determine the overall, LCR, and LWR temperature-decline rates. Evaporation rates of LCR and LWR regions were determined from the measured LCR and LWR temperature data using the physical model of Dursch et al.

Results. Twenty subjects completed the study. Mean (SD) difference of LCR temperature-decline rate was −0.08 (0.07)°C/s faster than LWR ($P < 0.0001$). Similarly, evaporation rates of LCR and LWR were statistically different ($P < 0.0001$). At ambient temperature, mean LCR and LWR evaporation rates were 76% and 27% of pure water evaporation flux, respectively. There was no statistically significant difference between the inter-day measured temperature-decline rates and the interblink starting temperature.

Conclusions. Significant differences in corneal temperature-decline rate and evaporation rate between LCR and LWR were quantified using infrared thermography. In agreement with literature, LCRs and LWRs correlate directly with fluorescein break-up areas and unbroken tear areas, respectively. Because lipid-evaporation protection is diminished in breakup areas, higher local evaporation rates and faster local cooling rates occur in LCRs relative to LWRs. Our results confirm this phenomenon clinically for the first time.

Keywords: dry eye, ocular surface temperature, thermography, evaporation, tear film, ocular surface cooling, evaporative cooling, ocular surface-temperature decline

The human tear film is composed of three major compartments: lipid coating layer, aqueous layer, and mucin adlayer.[1] A healthy lipid layer retards evaporation of the aqueous layer to keep the corneal surface hydrated during the interblink period.[2] However, lipid-layer structure and thickness during an interblink period are inhomogeneous across the corneal surface.[3,4] This nonuniformity, along with break-up of the thin lipid layer, leads to increased local evaporation rate, tear rupture, and hyperosmolarity in the ruptured regions.[5,6] Theoretical studies reveal that the localized osmolarity in thinning breakup spots can increase to at least 500 milliosmolar (mOsM) during an interblink due to the evaporation of the aqueous under layer.[5,7] Increased osmolarity causes discomfort to the enervated cornea; the prolonged state of this discomfort/pain throughout the day is commonly diagnosed as evaporative dry-eye disease.[8,9]

To assess evaporative dry-eye disease, clinicians commonly instill fluorescein dye on the ocular surface and measure the time it takes for a black spot to first form under fluorescent light.[10] Deepening and expanding black spots and streaks increase fluorescein concentration in the localized-thin black regions because of high local evaporation from the thinning aqueous-layer depressions.[11] First appearance of black spots after fluorescein instillation gives rise to a recorded fluorescein break-up time (FBUT).

One noninvasive method proposed in the literature to understand evaporative dry-eye disease is to measure the transient reduction in corneal surface temperature from infrared thermography.[12–14] Corneal surface-temperature decline during an open eye period is due to larger evaporative, radiative, and convective heat losses from the eye than heat gained from the anterior chamber and limbus.[12,15–20] Because radiative and convective heat losses on the ocular surface are expected to be uniform across the ocular surface in a given environment, localized differences in temperature of the corneal surface are assuredly due to differences

in localized evaporation rates. Simultaneous thermal and fluorescein break-up area recordings of Li et al.[16] confirm that infrared dark spots (i.e. cold) and fluorescein black break-up areas (i.e. ruptured aqueous film) directly correspond to each other. Abridging the observations of Li et al.[16] is the theoretical work of Peng et al.[5] These researchers established that lipid-layer break up diminishes the lipid layer insulating ability. Lessened insulation increases the local evaporation rate which results in cold high-evaporation areas in the corresponding fluorescein tear-film break-up areas. Peng et al.[5] and Braun et al.[7] establish that high evaporation areas result in high tear osmolarity, thus, connecting lipid layer break-up, cold spots, hyperosmolarity, and fluorescein break-up areas. Further, Dursch et al.[15] successfully predicted average corneal surface-temperature decline using measured increasing breakup areas and heat transfer theory. These authors imposed evaporation rates of pure water inside tear-breakup areas and calculated a reduced evaporation rate outside tear-breakup regions of between 50% and 95% depending on the individual subject. These combined works suggest that corneal surface-temperature history is a potential diagnostic of evaporative dry-eye disease because fluorescein break-up time differs significantly between healthy patients and dry-eye patients.[21]

Other published studies also found that dry-eye patients have faster rates of corneal surface temperature decline than do healthy eyes.[22–26] Further, Efron et al.[27] showed that subjects with slower rates of temperature decline are more likely able to keep their eyes open longer. However, existing studies on corneal surface temperature focus on overall average corneal surface temperature and not the temperatures in localized colder regions (LCRs) and in localized warmer regions (LWRs) that exist over the corneal surface.[15,16,22–26] In this study, we investigate how corneal temperature-decline rates differ in thinning localized breakup regions (i.e. LCRs) and along intact tear-film regions (i.e. LWRs). For the first time, we determine how evaporation rates differ between the two regions based on differing localized temperature-decline rates.

Methods

In ophthalmic literature, the cooling rate is often interpreted as how fast the temperature changes per unit time (e.g. in units of °C/s). However, the term "cooling rate" means energy lost per unit time (e.g. Joules/s). To avoid confusion, the term "temperature-decline rate" is adopted in this paper to describe temperature change per unit time. In addition, the phrase "evaporation rate" used here strictly refers to a rate of mass loss per unit area or a mass flux.

Study Protocol

Subjects were recruited from the University of California – Berkeley, and the surrounding community. All subjects were 18 years of age or older, had visual acuity correctable to 20/40 or better, were free of any ocular surface pathology, and were not taking ocular medications or systemic medications with ocular manifestations. Subjects discontinued contact-lens wear and use of any eye drops for at least 24 hours before each visit. Informed consent was received from all study participants after they were informed of the procedures, goals, and risks of the study. The study protocol was approved by the Committee for Protection of Human Subjects of the University of California – Berkeley, and followed the tenets of the Declaration of Helsinki.

Four measurements were made for each subject with repeat measurements taken on separate days. Each visit was scheduled at least 1 week apart from the previous visit, and all appointment times were scheduled 2 hours after subject's wake time. Room temperature and humidity were measured every visit using a combination digital thermometer and hygrometer (General Tools & Instruments, Secaucus, NJ, USA). Examination-room temperature and relative humidity were measured for each subject visit. Slit-lamp (SL120; Carl Zeiss Meditec Inc., Jena, Germany) examination was also performed at the beginning of each visit to ensure a healthy ocular surface. Subjects were acclimated to the ambient room environment for a minimum of 10 minutes prior to the corneal surface-temperature measurement.

Ocular surface-temperature history of the right eye was recorded at each visit using a FLIR A655sc Infrared Thermographer (FLIR Systems, Inc., Wilsonville, OR, USA). The thermographer has a thermal sensitivity of <0.03°C and a 17 µm pixel size.[28] Subjects were instructed to close their eyes for 2 minutes prior to recording the ocular surface-temperature history to ensure that the starting corneal temperature closely reached steady state.[15,16]

During recording, subjects were asked to keep their eyes open for as long as they comfortably could and to focus on the center of the camera to minimize eye movement. Obtained recordings were analyzed using ResearchIR 4.40.8 software (FLIR Systems, Inc., Wilsonville, OR, USA) to determine the corneal-surface temperature-decline rates.

Instrument software allowed a single operator to specify a local region of interest to examine containing approximately 4000 to 7000 pixels from the last frame of the interblink period for each measured eye. As illustrated in Figure 1, regions chosen to examine correspond to localized dark breakup areas and localized light non-breakup areas. Within each specified corneal region, the same operator randomly determined 3 unique dark and light spots each of size of 3-by-3-pixel area. Because each pixel provides a temperature value, LCRs and LWRs can be classified. Temperature values within the LCR and LWR regions were averaged to specify temperature-decline rates in the local cold and warm areas, as illustrated in Figure 2. In agreement with the clinical observations of Li et al.[16] and with the tear-film breakup theory of Peng et al.,[5] we thus establish that cold regions correspond to black-spot breakup areas and warm regions correspond to continuous non-breakup areas.

Statistical Analysis

Figure 2 provides an example of temperature histories and linear regression slopes of LCRs inside black spots (blue circles), LWRs outside black spots (red circles), and overall average cornea (black circles) for a single subject's eye. Linear regression of the measured histories gives the best-fit straight line, shown as a dashed line in Figure 2. The slope of the best-fit straight line defines the temperature-decline rate. Three localized corneal surface-temperature decline rates of LCRs and LWRs were averaged, respectively, to determine the reported average temperature-decline rate for colder breakup areas and warmer non-ruptured tear regions. A *t*-test, assuming unequal variance with 95% confidence interval, was performed to assess whether the straight-line temperature-fit slopes for LCR and LWR were statistically different. Temperature-declines rates of the LCRs and

Investigative Ophthalmology & Visual Science

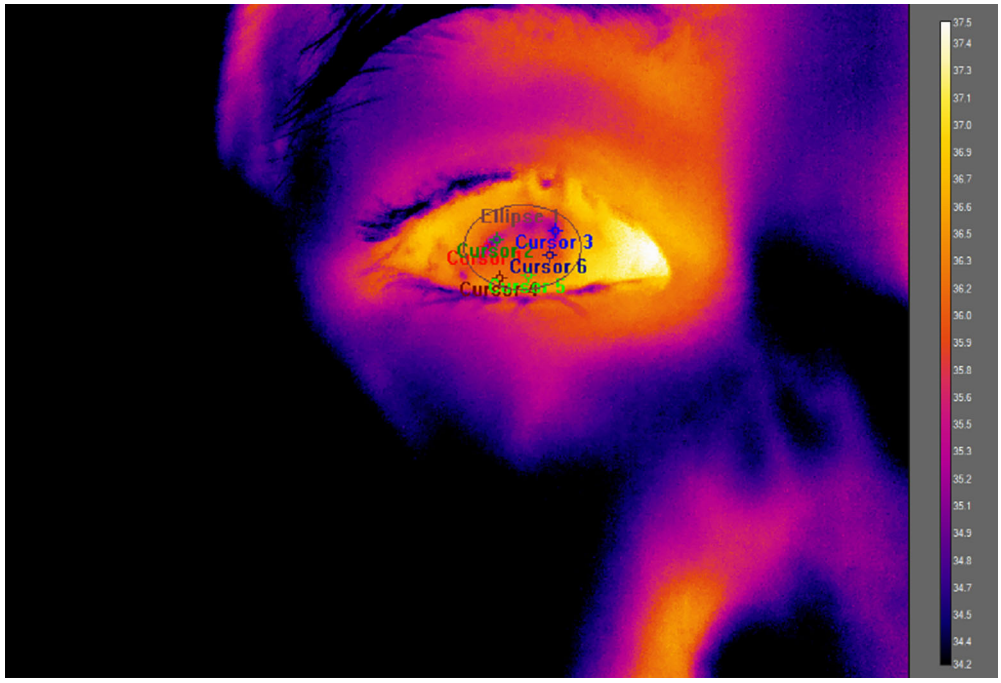

Figure 1. Example of localized and overall corneal regions of interest. Cursors 1 through 3 are the localized colder black-spot regions, whereas cursors 4 through 6 are localized non-black warmer regions. The ellipse demarks the corneal region of interest determined by the operator. The dark (cold) and light (warm) regions were determined from the frame before the subject started to close their eyes.

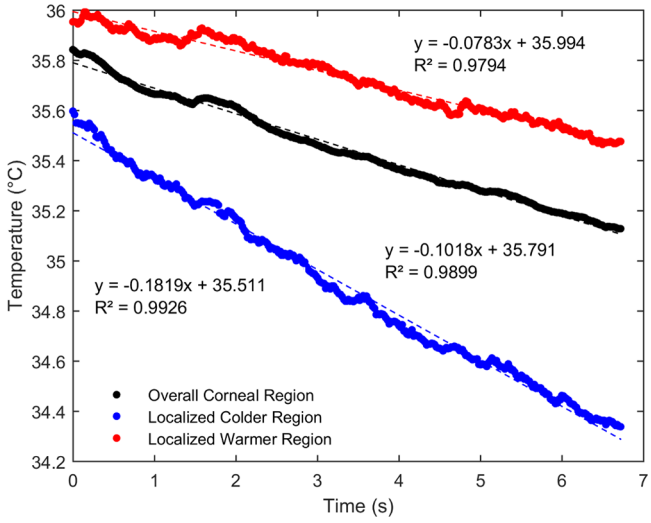

Figure 2. Example of temperature history of the average overall corneal (black), localized colder (blue), and localized warmer (red) regions from subject 6 visit 2. *Solid circles* represent measured data and the *dashed lines* represent the linear regression. Slopes obtained from linear lines represent the temperature-change rate. R^2 values are greater than 0.8 indicating good fits for the measurements. Localized colder black-spot regions exhibit lower starting temperature and faster temperature-change rate than localized non-black warmer regions.

LWRs were also compared by Limits of Agreement and the difference-versus-means plots.[29]

Importantly for later analysis, starting corneal surface temperatures of the cold and warm spots were also recorded along with the determined corneal surface-temperature rates. Three corneal surface temperatures at LCRs and LWRs at the beginning of the interblink period were likewise averaged, respectively, to compare the two tear regions' starting temperatures. The differences in the interblink starting corneal surface temperature of localized regions were also compared using the above statistical methods. To assess the inter-day repeatability of the interblink starting corneal surface temperature and temperature-decline rate, visits one and two data for each subject were averaged and compared with that of averaged data from visits three and four using Limits of Agreement and difference-versus-means plots.

Localized Evaporation-Rate Determination

The studies of Dursch et al.[15] and Li et al.[16] establish quantitatively that the decline in ocular surface temperature is the result of convective, radiative, and evaporative cooling. Of the three contributions, evaporative cooling is the major source of heat loss. This loss can vary significantly from subject to subject even in a controlled environment due to thickness/composition variances in the tear-film insulating lipid layer.[5] By imposing energy conservation (equations 2 and A8 of Dursch et al.[15]), initial surface temperature and best-fit temperature-decline rates of localized black-spot areas (i.e. LCRs) and localized lighter continuous tear-film areas outside black spots (i.e. LWRs; see Fig. 2), are re-expressed from theory analysis into local evaporation rates, for example, in kg/m^2/s. Details are found in the Supplementary information.

Evaporation rates of LCRs and LWRs are also reported here as fractional reductions of tear-film evaporation flux compared to that of pure water, as signified by the symbol β (see the Supplementary information for detailed information on assessment of β).[15] $\beta = 1$ is equivalent to pure water evaporation rate whereas $\beta = 0$ is equivalent to no evap-

Investigative Ophthalmology & Visual Science

oration. Said differently, $\beta = 1$ corresponds to no insulation by the tear-film lipid layer, whereas $\beta = 0$ corresponds to complete insulation by the tear-film lipid layer. Thus, by measuring localized temperature declines, the insulating effectiveness is assessed for a subject's lipid layer in both ruptured (LCR) and intact tear film (LWR).

Results

Of the 22 subjects that successfully completed the study, 20 subjects (2 men and 18 women, mean [SD] age = 23.05 [3.47] years) provided data usable for the analysis. One (1) subject did not complete the study; the data file from another subject was corrupted. With 4 visits, there were 80 pairs of corneal surface temperature-decline rates for LCR and LWR and 80 corneal-surface temperature-decline rates for overall corneal regions. Similarly, there were also 80 starting interblink temperatures for LCR, LWR, and overall corneal regions. Study demographics consisted of 11 Asians, 4 Caucasians, 1 African American, 2 Hispanics, and 2 others. All subjects were habitual contact-lens wearers. Descriptive statistics for corneal surface temperature-decline rates and interblink start temperatures for LCR, LWR, and overall corneal regions are provided in Table 1 along with the examination-room temperature and relative humidity. LCR black-colored regions occurred randomly throughout the central and peripheral cornea with LWR non-ruptured tear regions encompassing the LCR regions.

Figure 3 shows a scatter box plot of corneal surface-temperature decline rates in LCR and LWR domains. The *t*-test evaluation shows statistically significant differences ($P < 0.0001$) in corneal surface-temperature decline rates between the two localized regions. Mean (SD) difference between the two regions is −0.08 (0.07)°C/s. Limits of Agreement were 0.06 to −0.21°C/s, and the difference-versus-means plot is highlighted in Figure 4. Five LWR data resulted in non-physical positive average corneal surface-temperature change rates, meaning that the corneal surface actually warmed up rather than cooled down. However, these change rates were small and within experimental error suggesting almost complete insultation by the lipid layer. Interestingly, a positive association was observed between the localized mean rates and rate differences (i.e. subjects with small average corneal surface-temperature decline rates exhibit more uniform temperature declines across the corneal surface), further indicating that those subjects with minor break-up areas exhibit lower evaporation rate. Differences in the interblink start temperatures for LWR and LCR are also statistically significant ($P = 0.0045$); this indicates temperature variation across the cornea at the beginning of each interblink period.

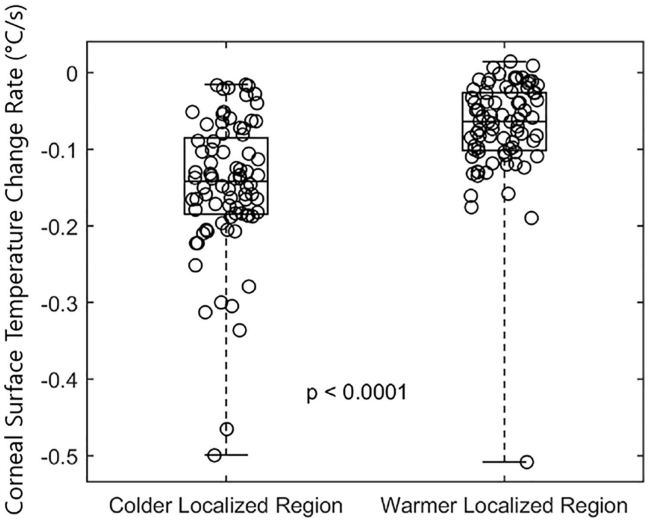

Figure 3. Scatter box plot of the corneal-surface temperature-decline rate. *Open circles* represent clinical localized temperature-decline rates. *Solid centered horizontal lines* are the median. There are 80 rates for colder and warmer localized regions each. Colder localized black-spot tear-rupture regions decline in temperature faster than do the warmer localized non-black tear-intact regions.

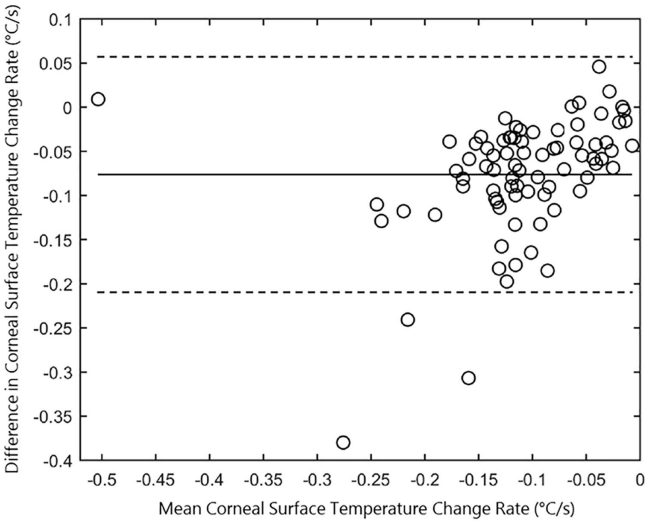

Figure 4. Difference-versus-mean plot for localized warmer and colder corneal surface-temperature change rates. A *solid horizontal line* indicates the mean difference of the localized corneal surface-temperature change rates. The *dashed horizontal line* marks the Limits of Agreement.

Table 1. Descriptive Statistics for the Four Visits

	Minimum	Maximum	Median	Mean	SD
Overall corneal-region temperature-decline rate, °C/s	−0.36	0.00	−0.10	−0.10	0.06
Localized colder region temperature-decline rate, °C/s	−0.50	−0.02	−0.14	−0.15	0.09
Localized warmer-region temperature-decline rate, °C/s	−0.51	0.01	−0.06	−0.07	0.07
Overall corneal-region temperature at the start of the interblink period, °C	33.79	36.70	35.52	35.54	0.58
Localized colder-region temperature at the start of the interblink, °C	33.60	36.60	35.35	35.36	0.61
Localized warmer-region temperature at the start of the interblink period, °C	33.90	36.77	35.63	35.63	0.56
Exam room temperature, °C	23.2	26.1	25.0	24.9	0.6
Exam room relative humidity, %	33.0	55.0	48.5	48.3	4.2

Investigative Ophthalmology & Visual Science

Table 2. Inter-day Repeatability Analysis for Overall Corneal Region and Localized Regions

	Mean Difference	SD	Limits of Agreement
Overall corneal-region temperature-decline rate, °C/s	0.01	0.05	[0.11 to −0.09]
Localized colder region temperature-decline rate, °C/s	0.00	0.08	[0.15 to −0.15]
Localized warmer region temperature-decline rate, °C/s	0.01	0.06	[0.13 to −0.11]
Overall corneal-region interblink starting temperature, °C	0.23	0.46	[1.14 to −0.68]
Localized colder region interblink starting temperature, °C	0.25	0.50	[1.23 to −0.73]
Localized warmer region interblink starting temperature, °C	0.22	0.49	[1.17 to −0.73]

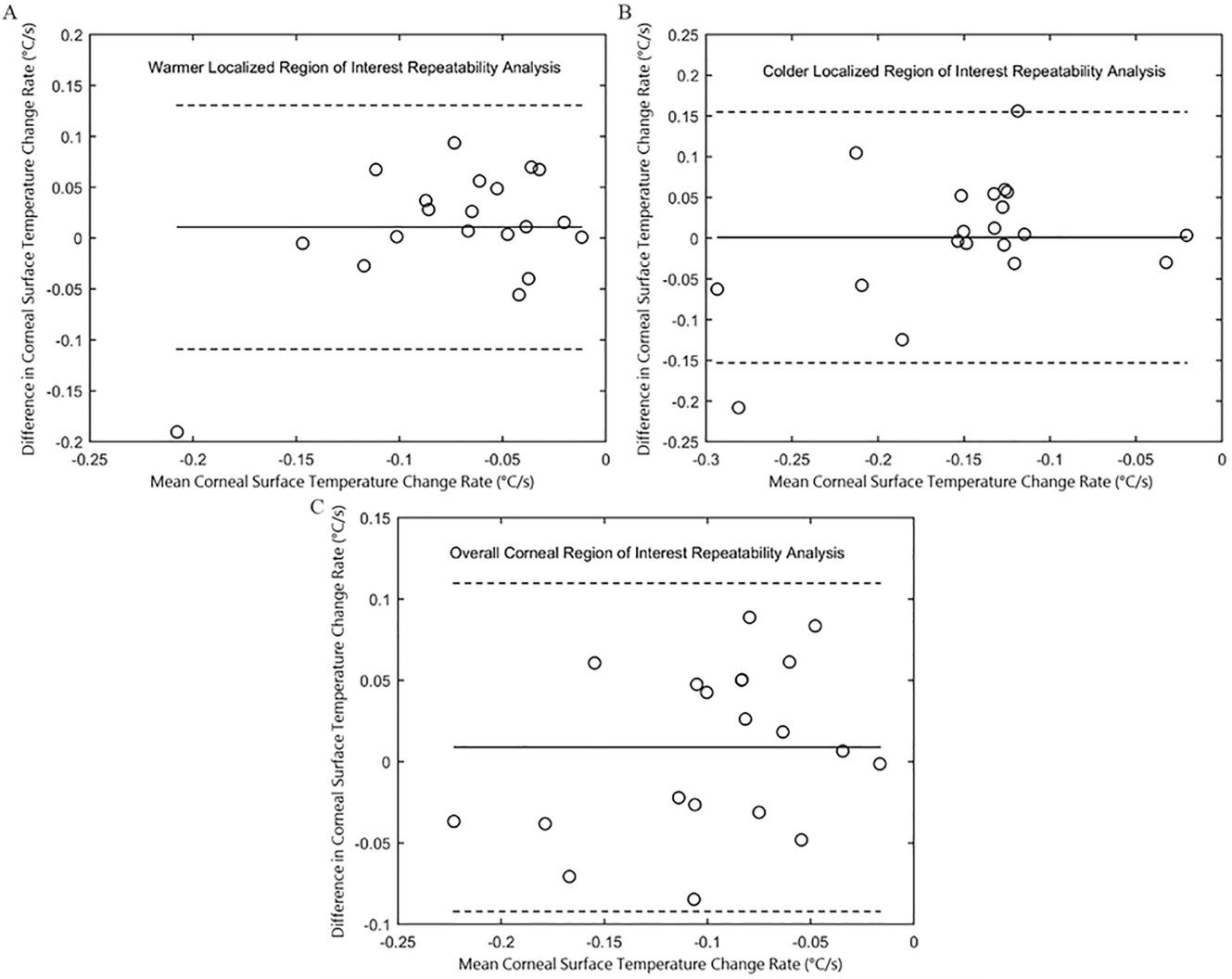

Figure 5. Difference-versus-mean plot for repeatability analyses. *Solid horizontal lines* indicate the mean difference of the localized corneal surface-temperature change rates. *Dashed horizonal lines* mark the Limits of Agreement. Panels (**A**, **B**, and **C**) are, respectively: localized non-ruptured-tear warmer regions, localized colder black-spot ruptured-tear regions, and overall cornea, respectively.

There is no significant difference in the corneal surface-temperature change rates between inter-day visits for the overall corneal region ($P = 0.6285$) and no significant difference in inter-day visit corneal surface-temperature change rates for LCR ($P = 0.9695$) and LWR ($P = 0.5488$). There is also no significant difference in the inter-day-interblink starting temperatures for the overall corneal region ($P = 0.1821$), LCR ($P = 0.1585$), and LWR ($P = 0.1890$). Inter-day mean difference, standard deviation, and Limits of Agreement for overall corneal surface temperature change rate, localized corneal surface temperature change rates, and interblink starting temperatures are provided in Table 2, again signifying insignificant differences in inter-day subject data. Difference-versus-mean plots provided in Figure 5 show no discernable corneal surface-temperature change rate trend for the overall corneal region, LCR, and LWR. Similarly, difference-versus-mean plots for the interblink starting temperature also showed no noticeable trend.

Figure 6 shows the scatter box plot of β (i.e. fraction of pure water evaporation rate) and of $\hat{f}_w$, the tear-film

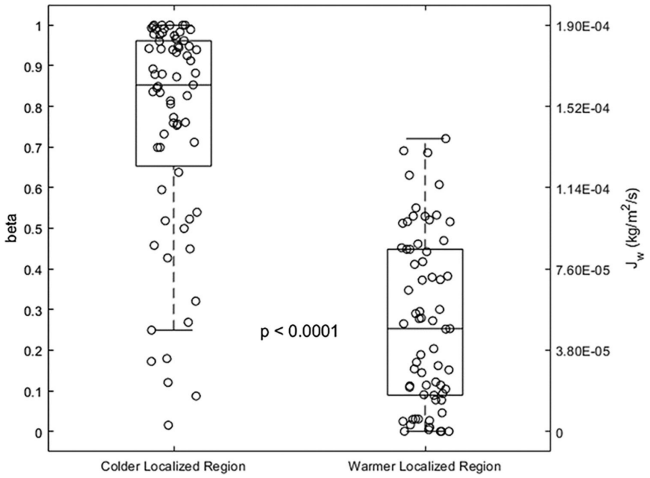

Figure 6. Scatter box plot of the β values (beta on left ordinate) for localized colder black-spot and warmer intact tear regions. Corresponding evaporation fluxes are provided on the right ordinate. *Open circles* represent each β value (and evaporation rate) determined from the clinical data; central lines locate the median. There are 67 sets of LCR and LWR measurements. Thirteen sets of LCR and LWR clinical data could not be used (see Results and Supplementary information).

Table 3. Descriptive Statistics for β

	Minimum	Maximum	Median	Mean	SD
Localized colder region β	0.02	1.00	0.85	0.76	0.27
Localized warmer region β	0.00	0.72	0.25	0.27	0.21

evaporation flux (kg/m^2/s), for LCR and LWR determined from measured subject data. Of the 80 pairs of LCR and LWR temperature data gathered, 13 pairs of measurements were not suitable to determine β due to some pairs of data having increased temperature change rate (5 pairs of data that indicate no evaporation). The remaining data (8 pairs of data) resulted in temperature change-rate differences between LCR and LWR that were too large to be explained by tear evaporation alone. These measurements are likely confounded by minor eye movement by the subjects. Table 3 provides the descriptive statistics of the determined β values. The *t*-test evaluation shows statistically significant differences in β ($P < 0.0001$) between LCR and LWR with a mean (SD) difference of 0.49 (0.30). Interestingly, even LCRs had a nonzero mean and median β values, meaning that tear-rupture regions exhibit some insulation causing slower evaporation rates than pure water.

Discussion

Clinically measured LCR and LWR temperature-decline rates in Figure 5 and heat-transfer model β values in Figure 6 both show statistically significant differences between ruptured and intact tear regions. In no subject was the β value smaller in the black-spot colder regions than in areas outside tear breakup. Thus, infrared thermography data indicate that formation of localized colder spots is driven by increased evaporation rates from those regions and that lipid layers in localized unstable rupture black spots do not inhibit water evaporation as well as those in the stable continuous tear regions of the corneal apical surface. Given the direct correlation between fluorescein break-up spots and ocular surface cold spots,[16] our study indicates that fluorescein-detected break-up spots are driven by increased localized evaporation rates. Equivalently, the evaporative-insulation by the lipid layer is not as effective in cold black-spot regions. These observations all strongly confirm the theory of Peng et al.[5] for how tear breakup occurs to rupture tear into deepening black spots. However, Li et al.[16] did not find universal association between fluorescein break-up spots and cold spots in every subject measurement. A possible reason is that these subjects exhibited excess tear production affecting fluorescein and/or temperature measurements. The lack of complete association requires further investigation.

Significant differences in the starting temperatures of LCR and LWR demonstrate that corneal surface temperature is not areally uniform at the beginning of an interblink cycle even after keeping the eyes closed for 2 minutes before taking the measurement.[15,16] It is possible that 2 minutes is not long enough for the corneal surface to reach an areally uniform steady-state temperature or that steady-state temperature at the beginning of the interblink period is innately non-uniform. Regardless, 2 minutes of eye closure is significantly longer than a typical blink time (i.e. approximately 0.3 seconds). Thus, in typical human-blinking behavior throughout the day, the corneal surface temperature is not uniform across the cornea even before the tear film starts to evaporate. This suggests that previous interblink tear-film break-up areas may influence the location of the subsequent interblink break-up areas.

Based on the authors' observations, LCRs formed randomly across the cornea throughout the interblink period and did not have a preference toward the central cornea. This indicates that the heat supply from the limbus, which causes the average peripheral cornea to be warmer than the central cornea,[12,20,30] does not overshadow the effect of evaporative cooling.

The observed mean β value of 0.27 for LWRs indicates that, on average, the intact lipid layer does not completely insulate tears from evaporating. Still in our study, tear lipid reduces tear evaporation rates by 70%, not far from that measured by Peng et al.[31] The measured mean β value of 0.76 for LCRs indicates that even for regions with high rates of evaporations in black rupture spots (i.e. in fluorescein-detected break-up areas), the aqueous layer does not evaporate at the rate of pure water, as assumed by Dursch et al.[15] This result suggests that there is some evaporation inhibition by the lipid layer even in areas that exhibit tear-film break up.[5,31]

To determine temperature-decline rates, the clinically measured temperature histories were best fit to straight lines by mean-square-error regression ($R^2 > 0.8$). The reason for the good linear fits is apparently because the corneal surface-temperature data are measured for a relatively short time interval (i.e. the interblink period). To remain consistent, the best linear fits are compared to theory-calculated temperature-versus-time plots to determine β values for each clinical temperature history, as outlined in the Supplementary information.

Subjects were asked to maintain their gaze at the camera center, but some minor eye movements were apparent from the recordings. These unintentional eye movements are a possible reason why there were five LWR data that showed a minor increase in temperature over time (within experimental error) and eight sets of data with large deviation in temperature-decline rate between LWR and LCR that cannot

Investigative Ophthalmology & Visual Science

be explained by evaporative cooling alone. Lateral tear flow due to surface-tension gradients is another possible explanation.[32] Nevertheless, both temperature-decline rates and determined β values of LWRs and LCRs were statistically different. Introducing eye tracking for future thermal studies will likely reduce the noise in the measured thermal data.

Another limitation is that the operator-determined overall corneal region may have not captured the entire cornea or may have captured parts of the limbus. This is due to the limitation of the infrared camera in detecting exactly where the cornea ends and where the limbus starts. Regardless of this limitation, the operator-determined overall corneal region is mostly that of the full cornea (see Fig. 1). Further improvement in determining the termination of the cornea and commencement of the limbus will better locate the overall corneal region.

Quantification of temperature-decline rates and evaporation rates of the cold spots provides a novel method to identify break-up spots on the corneal surface. Further investigation is necessary to ascertain whether localized evaporation rates and temperature-decline rates of cold and/or warm areas correlate with dry-eye symptoms before infrared thermography can be used as a diagnostic tool for dry eyes. Surface area of LCR and LWR regions (i.e. area size and growth)[15,16] and number of LCR and LWR regions during an interblink period, which were not investigated in this study, may play critical roles and need to be investigated further.[6,33] Nevertheless, we demonstrate here first that local evaporation rates play a determinant role in tear-film breakup[5,16]; second, that localized evaporation rates and temperature-decline rates vary significantly in a given interblink period and that these rates can be determined for tear-film breakup areas using infrared thermography. For the first time, we establish clinically that tear-rupture areas in tear films exhibit larger temperature-decline rates and higher evaporation rates than that of the surrounding continuous tear film. This conclusion strongly supports previous works suggesting that tear-film breakup is driven by local lipid instabilities[5,6,32,34,35] leading to locally high tear evaporation rates, tear rupture, and increased osmolarities.[5,6]

Acknowledgments

The authors thank Kayla Panora for initiating the theory calculations.

Financial support was provided from the Roberta J. Smith Foundation and UCB CRC Unrestricted Fund. (M.C.L.).

Disclosure: **Y.H. Kim**, None; **J. Lee**, None; **S.M. Yi**, None; **M.C. Lin**, None; **C.J. Radke**, None

References

1. Mathers WD, Lane JA. Meibomian gland lipids, evaporation, and tear film stability. In: Sullivan DA, Dartt DA, Meneray MA, eds. *Lacrimal Gland, Tear Film, and Dry Eye Syndromes 2*. New York, NY: Springer; 1998:349–359.
2. Cerretani CF, Radke CJ. Tear dynamics in healthy and dry eyes. *Curr Eye Res*. 2014;39(6):580–595.
3. Doane MG. Abnormalities of the structure of the superficial lipid layer on the in vivo dry-eye tear film. In: Sullivan DA, ed. *Lacrimal Gland, Tear Film, and Dry Eye Syndromes. Advances in Experimental Medicine and Biology*, Vol 350. New York, NY: Springer; 1994:489–493.
4. Cwiklik L. Tear film lipid layer: a molecular level review. *Biochim Biophys Acta*. 2016;1858(10):2421–2430.
5. Peng CC, Cerretani CF, Braun RJ, Radke CJ. Evaporation-driven instability of the precorneal tear film. *Adv Colloid Interface*. 2014;206:250–264.
6. Liu H, Begley C, Chen M, et al. A link between tear instability and hyperosmolarity in dry eye. *Invest Ophthalmol Vis Sci*. 2009;50(8):3671–3679.
7. Braun RJ, King-Smith PE, Begley CG, Li L, Gewecke NR. Dynamics and function of the tear film in relation to the blink cycle. *Prog Retin Eye Res*. 2015;45:132–164.
8. Johnson ME, Murphy PJ. Changes in the tear film and ocular surface from dry eye syndrome. *Prog Retin Eye Res*. 2004;23(4):449–474.
9. Lucca JA, Nunez JN, Farris RL. A comparison of diagnostic tests for keratoconjunctivitis sicca: lactoplate, Schirmer, and tear osmolarity. *CLAO J*. 1990;16:109–112.
10. Abelson MB, Ousler GW, Nally LA, Welch D, Krenzer K. Alternative reference values for tear film break up time in normal and dry eye populations. In: Sullivan DA, Stern ME, Tsubota K, Dartt DA, Sullivan RM, Bromberg BB, eds. *Lacrimal Gland, Tear Film, and Dry Eye Syndromes 3*. New York, NY: Springer; 2002.
11. Nichols JJ, King-Smith PE, Hinel EA, Thangavelu M, Nichols KK. The use of fluorescent quenching in studying the contribution of evaporation to tear thinning. *Invest Ophthalmol Vis Sci*. 2012;53(9):5426–5432.
12. Craig JP, Singh I, Tomlinson A, Morgan PB, Efron N. The role of tear physiology in ocular surface temperature. *Eye*. 2000;14:635–641.
13. Morgan PB, Tullo AB, Efron N. Ocular surface cooling in dry eye: a pilot study. *J Br Contact Lens Assoc*. 1996;19:7–10.
14. Morgan PB, Tullo AB, Efron N. Infrared thermography of the tear film in dry eye. *Eye*. 1995;9:615–618.
15. Dursch TJ, Li W, Taraz B, Lin MC, Radke CJ. Tear-film evaporation rate from simultaneous ocular-surface temperature and tear-breakup area. *Optom Vis Sci*. 2018;95(1):5–12.
16. Li W, Graham AD, Selvin S, Lin MC. Ocular surface cooling corresponds to tear film thinning and breakup. *Optom Vis Sci*. 2015;92(9):e248–e256.
17. Ooi EH, Ng E. Ocular temperature distribution: a mathematical perspective. *J Mech Med Biol*. 2009;9:199–227.
18. Ooi EH, Ng EYK. Effects of natural convection within the anterior chamber on the ocular heat transfer. *Int J Numer Method Biomed Eng*. 2010;27(3):408–423.
19. Ooi EH, Ng E. Simulation of aqueous humor hydrodynamics in human eye heat transfer. *Comput Bio Med*. 2008;38:252–262.
20. Li L, Braun RJ. A model for the human tear film with heating from within the eye. *Phys Fluids*. 2012;24:062103.
21. Paugh JR, Tse J, Nguyen T, et al. Efficacy of the fluorescein tear breakup time (TBUT) test in dry eye. *Cornea*. 2020;39(1):92–98.
22. Fujishima H, Toda I, Yamada M, Sato N, Tsubota K. Corneal temperature in patients with dry eye evaluated by infrared radiation thermometry. *Br J Ophthalmol*. 1996;80:29–32.
23. Kamao T, Yamaguchi M, Kawasaki S, Mizoue S, Shiraishi A, Ohashi Y. Screening for dry eye with newly developed ocular surface thermographer. *Am J Ophthalmol*. 2011;151:782–791.
24. Su TY, Hwa CK, Liu PH, et al. Noncontact detection of dry eye using a custom designed infrared thermal image system. *J Biomed Opt*. 2011;16(4):046009.
25. Wolffsohn JS, Arita R, Chalmers R, et al. TFOS DEWS II diagnostic methodology report. *Ocul Surf*. 2017;15(3):539–574.
26. Craig JP, Singh I, Tomlinson A, Morgan PB, Efron N. The role of tear physiology in ocular surface temperature. *Eye*. 2000;14:635–641.

27. Efron N, Young G, Brennan NA. Ocular surface temperature. *Curr Eye Res*. 1989;8(9):901–906.
28. Teledyne FLIR. High-resolution science grade LWIR Camera FLIR A655sc. Published 2024. Accessed June 16, 2024. Available at: https://www.flir.com/products/a655sc/?vertical=rd+science&segment=solutions.
29. Bland JM, Altman DG. Agreement between methods of measurement with multiple observations per individual. *J Biopharmaceutical Statistics*. 2007;17:571–582.
30. Aliò J, Padron M. Influence of age on the temperature of the anterior segment of the eye. *Ophthalmic Res*. 1982;14(3):153–159.
31. Peng CC, Cerretani CF, Li Y, et al. Flow evaporimeter to assess evaporative resistance of human tear-film lipid layer. *Ind Eng Chem Res*. 2014;53(47):18130–18139.
32. King-Smith PE, Reuter KS, Braun RJ, Nichols JJ, Nichols KK. Tear film breakup and structure studied by simultaneous video recording of fluorescence and tear film lipid layer images. *Invest Ophthalmol Vis Sci*. 2013;54(7):4900–4909.
33. Creech JL, Do LT, Fatt I, Radke CJ. In vivo tear-film thickness determination and implications for tear-film stability. *Curr Eye Res*. 1998;17(11):1058–1066.
34. King-Smith PE, Nichols JJ, Nichols KK, Fink BA, Braun RJ. Contributions of evaporation and other mechanisms to tear film thinning and break-up. *Optom Vis Sci*. 2008;85:623–630.
35. Kimball SK, King-Smith PE, Nichols JJ. Evidence for the major contribution of evaporation to tear film thinning between blinks. *Invest Ophthalmol Vis Sci*. 2010;51:6294–6297.

Investigative Ophthalmology & Visual Science